

Article

# Effect of WC Nanoparticles on the Microstructure and Properties of WC-Bronze-Ni-Mn Based Diamond Composites

Siqi Li <sup>1,2</sup>, Zhe Han <sup>1,2</sup>, Qingnan Meng <sup>1,2</sup>, Xinzhe Zhao <sup>1,2</sup>, Xin Cao <sup>1,2</sup> and Baochang Liu <sup>1,2,3,\*</sup>

<sup>1</sup> College of Construction Engineering, Jilin University, Changchun 130026, China; siqi17@mails.jlu.edu.cn (S.L.); hanzhe17@mails.jlu.edu.cn (Z.H.); qingnanmeng@jlu.edu.cn (Q.M.); zhaoxz17@mails.jlu.edu.cn (X.Z.); caoxin16@mails.jlu.edu.cn (X.C.)

<sup>2</sup> Key Laboratory of Drilling and Exploitation Technology in Complex Conditions of Ministry of Natural Resources, Changchun 130026, China

<sup>3</sup> State Key Laboratory of Superhard Materials, Changchun 130021, China

\* Correspondence: liubc@jlu.edu.cn; Tel.: +86-431-8850-2891

Received: 24 July 2018; Accepted: 25 August 2018; Published: 1 September 2018



**Abstract:** Metal matrix-impregnated diamond composites are widely used for fabricating diamond tools. In order to meet the actual engineering challenges, researchers have made many efforts to seek effective methods to enhance the performance of conventional metal matrices. In this work, tungsten carbide (WC) nanoparticles were introduced into WC-Bronze-Ni-Mn matrix with and without diamond grits for improving the performance of conventional impregnated diamond composites. The influence of WC nanoparticles on the microstructure, densification, hardness, bending strength and wear resistance of matrix and diamond composites were investigated. The results showed that the bending strength of matrix increased up to approximately 20% upon nano-WC addition, while densification and hardness fluctuate slightly. The grinding ratio of diamond composites increased significantly by about 100% due to nano-WC addition. The strengthening mechanism was proposed according to experimental results. The diamond composites with 2.8 wt% nano-WC addition exhibited the best overall properties, thus having potential to apply to further diamond tools.

**Keywords:** WC nanoparticles; metal matrix; impregnated diamond composites; wear resistance

## 1. Introduction

Impregnated diamond composites produced by powder metallurgy are widely used for fabricating tools employed in cutting, drilling, milling and polishing applications [1–4]. The choice of the matrix materials which holds the diamond is essential to properties and service life of diamond tools [5,6]. WC-Bronze-Ni-Mn matrix, a composite mainly containing micron-WC, bronze (Cu85%-Sn6%-Zn6%-Pb3%) alloy, Ni and Mn, is widely used for diamond drilling tool manufacturing [7,8]. The micro-WC is used as framework material to enhance hardness and wear resistance, bronze is used as bonding phase, the element of Ni is used as strengthened phase because of its excellent wettability with diamond and Mn plays the role of antioxidant [9]. WC-Bronze-Ni-Mn matrix has high strength and adjustable properties that is suitable for different rock types, the diamond grits in tools can contact the rocks more easily and maintain an abrasive cutting surface between tools and rocks. The matrix properties and wear rate difference between matrix and diamond grits are important factors determining the performance of diamond tools [10–12]. Harsh and complex service conditions such as hydro-abrasive wear, impact stress and elevated temperature, require the development of new matrix materials with enhanced mechanical properties and wear resistance [13]. Different kinds of metals, such as Co, Fe and Ni, have been served as matrix materials for production

of diamond tools [14–17]. However, the actual applicability of these matrices based diamond tools for different rocks is unsatisfactory because they wear out faster than diamond grits when processing hard and abrasive rocks. These metals also catalyze the reaction of diamond (sp<sup>3</sup>) to graphite (sp<sup>2</sup>) at elevated temperature, which reduces adhesion between diamond and matrix [18–20].

Development of metal matrix composites reinforced by nanoparticles is a promising way to meet the actual engineering requirement on mechanical and tribological properties. Metal matrix composites reinforced by nanoparticles have promising properties, which is more suitable for a large number of functional and structural applications than other metal matrix strengthening methods, such as solution strengthening, work hardening and precipitation strengthening [14]. Recently, some researchers investigated metal matrix reinforced with nano-particles (nanotubes), finding out that adding nanosized reinforcement improved hardness, bending strength and wear resistance of matrix [21–28]. Ceramic (Al<sub>2</sub>O<sub>3</sub>, ZrO<sub>2</sub>, TiC, TiB<sub>2</sub>, WC, etc.) nanoparticles can be used as reinforcing phase. But Al<sub>2</sub>O<sub>3</sub>, ZrO<sub>2</sub>, TiC and TiB<sub>2</sub> nanoparticles have low wettability with bonding phase bronze, which decreases composites properties [7,13,22–26]. WC nanoparticles have excellent wettability with bronze and have good properties, namely high hardness, high wear resistance, good thermal and chemical stability. So it has been used in enhancing Ni, Fe and Co based matrix composites for cutting tools and modifying coatings for high wear resistance tools [13,22,29–31].

In this work, nano-WC was introduced into WC-Bronze-Ni-Mn based diamond composites for the first time. The effects of nano-WC addition on the microstructures, mechanical properties, and wear resistance of WC-Bronze-Ni-Mn based diamond composites were investigated and discussed. The aim is to seek optimal nano-WC addition concentration to meet the requirement of mechanical properties and wear resistance.

## 2. Materials and Methods

### 2.1. Sample Preparation

The composition of initial matrix in this work is given in Table 1, including WC (99.9% purity, Zhuzhou, China), bronze (99.9% purity, Beijing, China), Ni (99.9% purity, Beijing, China) and Mn (99.9% purity, Beijing, China).

**Table 1.** Composition of initial matrix.

Composition	WC	Bronze	Ni	Mn
Content (wt%)	55	35	5	5
Average particle size (μm)	10	50	75	60

Two series of samples (size: 38 × 8 × 5 mm<sup>3</sup>), matrix and impregnated diamond composites samples, were fabricated by power metallurgy methods of hot-pressing sintering. For purpose of obtaining uniform mixture, initial matrix powder was first mixed in a ball milling machine (Focucy, P400, Changsha, China) with WC balls for 24 h at a speed 120 rpm. Nano-WC (99.9% purity, average particle size of 80 nm, Qinhuangdao, China) with different mass percent concentration were then mixed with initial powder that was milled already using the same ball milling machine for 8 h at a speed 120 rpm. The resultant mixture with various concentration of nano-WC were sintering by hot-pressing in graphite moulds at 980 °C for 5 min. During the sintered process, the samples were forced by a uniaxial pressure of 35 MPa. The sintering apparatus was an intermediate frequency furnace (KGPS, Ezhou, China).

In impregnated diamond samples preparation process, initial matrix powder and different mass percent concentration nano-WC were mixed by the same way as matrix samples. The diamond grits (20 vol% concentration, synthetic, 270–325 μm, Changge, China) were added into the resultant mixture through a three-dimension mixer (JH2D-6, Zhengzhou, China) for 4 h. The diamond composites samples were prepared by hot-pressing sintering at the same parameters as matrix samples.

## 2.2. Characterization

The density of samples was measured by high precision density tester (Dahometer, DE-120M) via Archimedes method. The Rockwell hardness scale C (HRC) tests were carried out using a Rockwell hardness tester (Huayin HRS-150, Yantai, China). Three-point bending strength was tested by an electronic universal test machine (DDL 100, CIMACH, Chuangchun, China). The microstructure of composites were characterized by SEM (Hitachi S-4800, Tokyo, Japan) equipped with an energy dispersive spectrometer (EDS) and the acceleration voltage of EDS mapping experiments was 25 kV.

Grinding ratio tests were performed using a grinding ratio measurement apparatus as illustrated in Figure 1. The SiC grinding wheel with the dimension of 100 mm diameter and 20 mm thickness was applied as wear counterparts. The testing parameters were as follows: linear velocity 15 m/s, load 500 g, swing frequency 30 min<sup>-1</sup> and grinding time > 100 s. The grinding ratio was calculated by the formula

$$Ra = \Delta Mg / \Delta Ms \quad (1)$$

where Ra is the sample grinding ratio;  $\Delta Mg$  is the weight loss of SiC grinding wheel;  $\Delta Ms$  is the weight loss of sample.

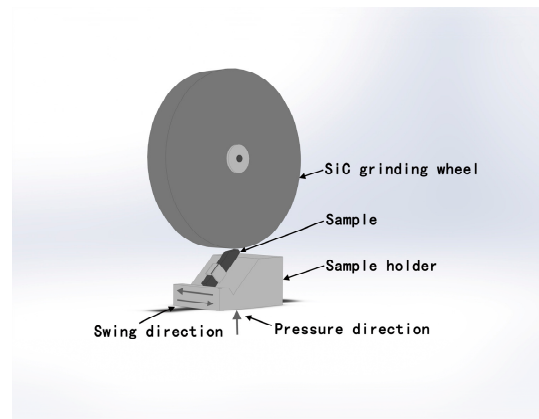


Figure 1. Schematic diagram of the grinding ratio test.

## 3. Results and Discussion

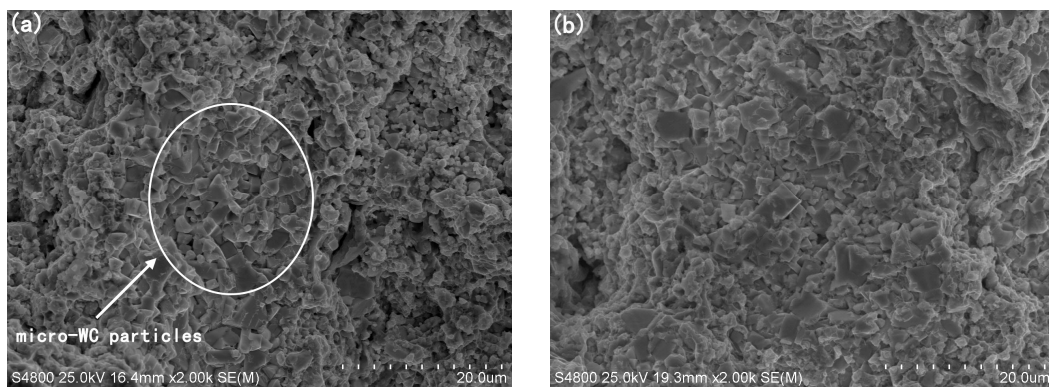
The designation, composition and mechanical properties of samples are summarized in Table 2.

Table 2. The designation, composition and mechanical properties of samples.

Samples	Composites	Relative Density (%)	Hardness (HRC)	Bending Strength (MPa)
S0	Matrix	98.4	42.2 ± 2.9	705.9 ± 35.4
S1	Matrix + 0.5 wt% nano-WC	97.0	36.9 ± 0.9	700.9 ± 30.3
S2	Matrix + 1.0 wt% nano-WC	97.0	36.7 ± 2.0	732.1 ± 16.6
S3	Matrix + 1.5 wt% nano-WC	97.8	39.2 ± 4.1	753.5 ± 31.0
S4	Matrix + 2.0 wt% nano-WC	97.6	36.2 ± 3.1	769.6 ± 29.9
S5	Matrix + 2.5 wt% nano-WC	98.5	40.7 ± 1.3	824.5 ± 28.4
S6	Matrix + 3.0 wt% nano-WC	98.3	38.8 ± 2.6	736.0 ± 24.5
SD0	Matrix + Diamond	95.8	-	391.0 ± 25.5
SD1	Matrix + 2.2 wt% nano-WC + Diamond	93.1	-	461.6 ± 32.0
SD2	Matrix + 2.5 wt% nano-WC + Diamond	94.8	-	398.8 ± 19.2
SD3	Matrix + 2.8 wt% nano-WC + Diamond	96.1	-	384.3 ± 7.4
SD4	Matrix + 3.1 wt% nano-WC + Diamond	95.3	-	398.0 ± 32.4

### 3.1. Microstructure

Sample S5 with 2.5 wt% nano-WC shows the optimum mechanical properties, so S5 and reference sample S0 are chose to be investigated. Figure 2 shows the fracture morphologies of matrix samples S0 and S5. In Figure 2a,b, the 0.5–6  $\mu\text{m}$  matrix grains can be differentiated according to their shape: polygon-shaped grains consisting of micron-WC particles [7–9,29–31] and smooth round grains around, which are bonding phases bronze and Ni. As marked in Figure 2a, micro-WC particles are discerned from bronze phase grains by means of shape. The particle size of micro-WC in Figure 2 is from 0.5 to 6  $\mu\text{m}$  that is not consistent with initial micro-WC particle size (10  $\mu\text{m}$ ). The ball milling process with WC balls is the reason of decrease in particle size. The ball milling machine (Focucy, P400, Changsha, China) is not a high energy ball mill and its main function is to mix powders evenly. So the wear amount of WC balls during ball milling process is extreme small and can not influence experimental results. Elements W, Cu, Ni and Mn show clear signals and uniform elemental distributions in EDS element mappings in Figure 3. The acceleration voltage used in EDS mapping experiments was 25 kV which correlates with a higher depth of analysis. So the element W is not clearly separated from other metals because the depth of analysis is larger than one layer particles.



**Figure 2.** The fracture morphologies of samples: (a) S0; (b) S5.

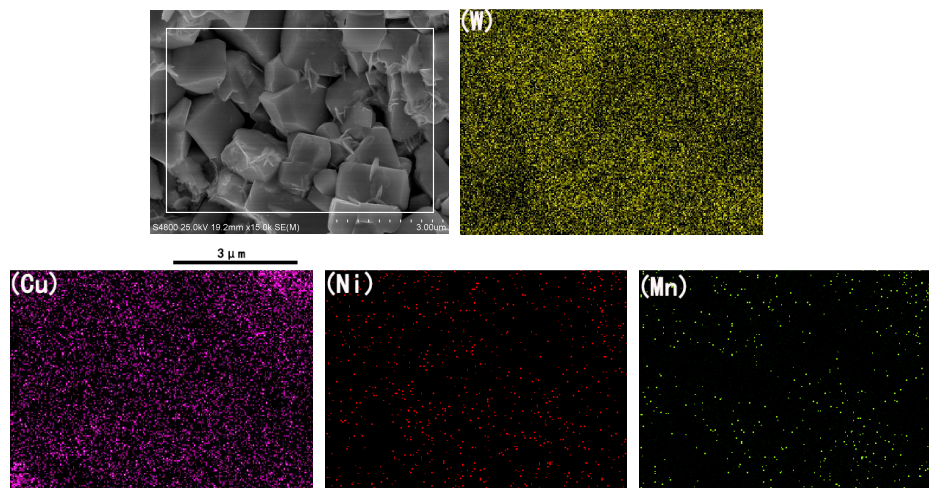


**Figure 3.** EDS element mappings of W, Cu and Ni for the fracture morphology of sample S5.

WC nanoparticles are found on fracture surface of sample S5 with 2.5 wt% nano-WC addition (Figure 4). The wettability between WC and bronze is excellent [9], so WC nanoparticles are wrapped by bronze phase during sintering process.

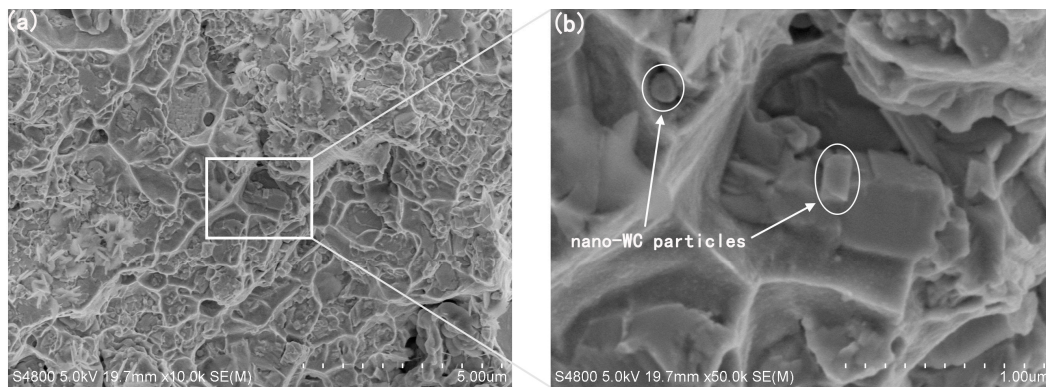


Figure 4. The fracture morphologies of sample: (a,b) S5.

SEM micrographs of impregnated diamond samples SD0 and SD1 are displayed in Figure 5. It shows that diamond grits are partially embedded in the matrix on fracture surfaces. As marked in Figure 5b,d, with the addition of 2.2 wt% nano-WC, the average width of the crack between diamond and matrix decreases from 4.1  $\mu\text{m}$  to 3.0  $\mu\text{m}$ . The smaller crack width means that the matrix holds diamond grits more firmly, which contributes positively to mechanical and tribological properties of impregnated diamond composites. The average width of the crack between diamond and matrix is shown in Table 3. The number of measured widths in the calculation of average is 15. With further increase of nano-WC addition, the influence on crack width is not significant. Some pores of SD1 found in Figure 5d have negative impact on relative density, which is consistent with the test results in Table 2. The pore existence states of sample SD2, SD3 and SD4 are similar to SD0.

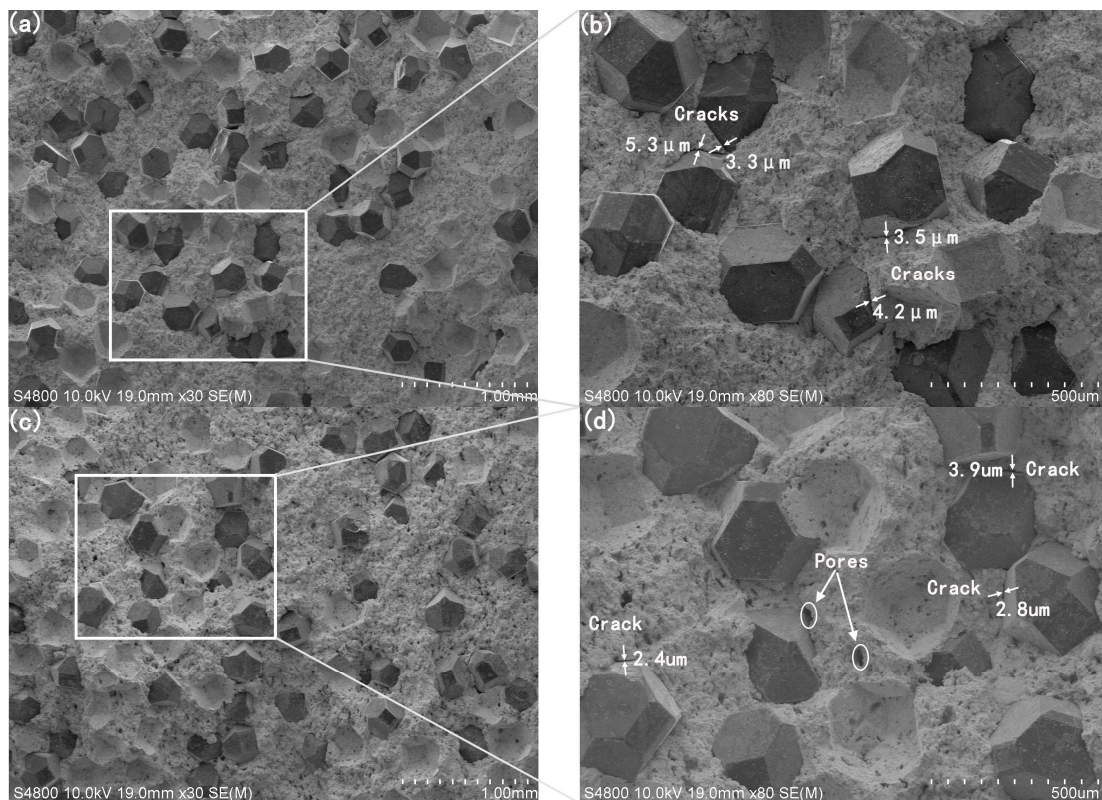


Figure 5. The fracture morphologies of samples: (a,b) SD0; (c,d) SD1.

**Table 3.** The average width of the crack between diamond and matrix of impregnated samples.

Samples	SD0	SD1	SD2	SD3	SD4
Width ( $\mu\text{m}$ )	4.1	3.0	3.8	4.0	4.2

### 3.2. Mechanical Properties

The mechanical properties of matrix samples are shown in Figure 6. With the increase of nano-WC particles addition, the relative density and hardness fluctuate and do not have significant changes (Figure 6a,b). It should be note that the introduction of nano-WC has little effect on relative density and hardness.

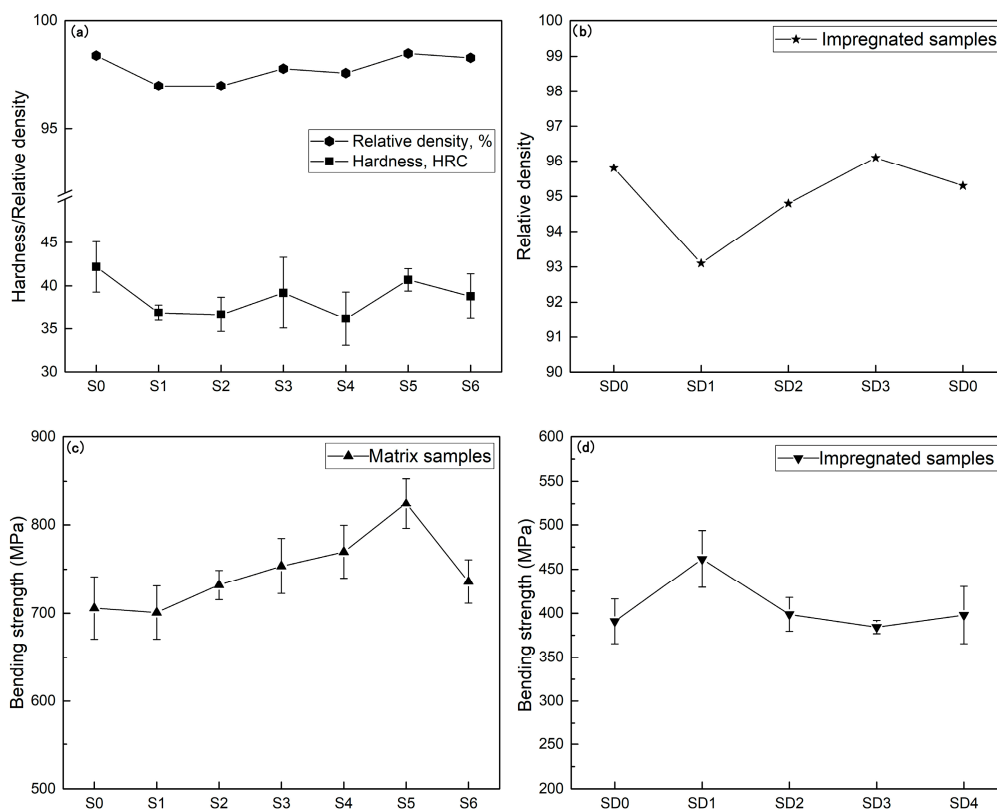


**Figure 6.** Mechanical properties of samples. (a) The relative density and HRC values of matrix samples; (b) The relative density of impregnated diamond samples; (c) The bending strength of matrix samples; (d) The bending strength of impregnated diamond samples.

Bending strength of matrix samples shows a trend of first increase and then decrease (Figure 6c), and sample S5 has the best value. The positive influence on bending strength of nano-WC addition can be associate with Orowan strengthening effect. The nano-WC particles pin the crossing dislocation and promote dislocations bowing around the particles under external load [32,33]. In addition, the mismatch in the coefficient of thermal expansion (CET) between WC ( $6 \times 10^{-6} \text{ K}^{-1}$ ) and bronze ( $\geq 18 \times 10^{-6} \text{ K}^{-1}$ ) needs further consideration [7,34]. During the cooling from processing temperature ( $980 \text{ }^\circ\text{C}$ ), thermal stresses around the nano-WC particles lead to plastic deformation, especially in the interface area [33]. These stresses decrease quickly with increasing distance from the boundary, generating dislocation defects in the close vicinity of nano-WC. A large amount of nanoparticles is benefited to enhance dislocation density, resulting in an improvement of the deformation resistance. While concentration of nano-WC goes higher than 2.5 wt%, agglomeration phenomenon weakens the reinforcement effect.

As illustrated in Figure 6d, the bending strength of impregnated diamond sample SD1 shows the peak value and the value of SD2, SD3 and SD4 is close to SD0. Combined with fracture SEM observation (Figure 5) and average crack width (Table 3), the width of the crack decreases from 4.1  $\mu\text{m}$  to 3.0  $\mu\text{m}$  after adding 2.2 wt% nano-WC. This structural feature indicates matrix of SD1 has good diamond-holding capability, which is benefited to the stress transfer, enhancing the bending strength. Diamond grits act as weakening phase during bending strength test, so the holding strength at the interfaces between diamond grits and matrix is a factor influencing diamond composites bending strength and overall performance [3,5]. The interface structure observed between diamond grits and matrix of sample SD2, SD3 and SD4 is similar to SD0, this is accordance with bending strength test results.

### 3.3. Wear Resistance

Grinding ratio is a measurement index for evaluating the wear resistance and tribological performance of diamond composites [11]. The results for grinding ratio of impregnated diamond samples with different mass percent concentration nano-WC are summarized in bar chart (Figure 7). The grinding ratio increases remarkably after adding WC nanoparticles, proving that nano-WC plays a significant role in wear resistance of impregnated diamond composites. The grinding ratio increases firstly and then decreases with nano-WC content increases and grinding ratio of sample SD3 shows an about 100% increase in comparison with SD0. The wear resistance of impregnated diamond composites is higher than other WC-based, Fe-based, Co-based and Ni-based diamond composites [7,8,21–23].

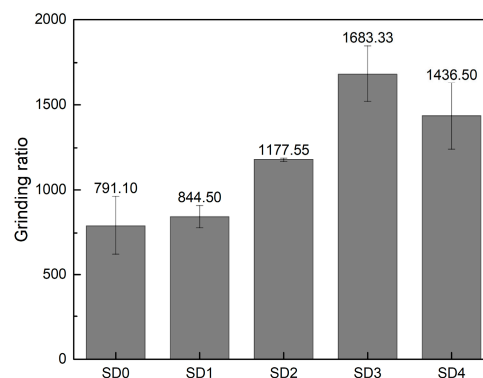


**Figure 7.** Results of grinding ratio test of impregnated diamond samples.

The diamond retention capacity largely determines the wear resistance of impregnated diamond composite [3]. As shown in Figure 4, WC nanoparticles are found on fracture surface, and these nanoparticles enhance the internal friction coefficient in the matrix as same as the friction coefficient between diamond grits and matrix [3,15]. Under complex and alternating cutting force, diamond grits show a tendency to rotate and then pull out of matrix easily. The increase of friction improves retentive capabilities of the matrix and reduces the rotating tendency, which enhances diamond retention in the matrix that is benefited to wear resistance of diamond composites. Hence, the grinding ratio of samples SD2, SD3 and SD4 with nano-WC addition is larger than reference one without nano-WC addition and SD3 with 2.8 wt% nano-WC has the best value. While concentration of nano-WC exceeds higher than 2.8 wt%, agglomeration phenomenon is harmful to the reinforcement effect.

The bending strength is also a factor affecting the wear resistance. The theoretical relationship between bending strength and wear resistance has been analyzed in the literatures [9–11]. A higher bending strength leads to a stronger support for diamond grits, meaning that diamond grits would not be lost permanently by pulling out when facing complex stresses conditions. But it can be found that the bending strength of SD1 is larger than SD0, SD2, SD3 and SD4 but the grinding ratio of SD1 with 2.2 wt% nano-WC is smaller than that of SD2, SD3 and SD4 and similar to SD0. This indicates

that other factors weaken the wear resistance of SD1. As evidenced in Figure 5d or Figure 6b, the low relative density of SD1 means it has high porosity. The high porosity of SD1 implies the matrix wears faster than other samples, which causes diamond grits to pull out of matrix more easily. So the low relative density results in the decrease of grinding ratio of SD1.

#### 4. Conclusions

The effect of WC nanoparticles on the microstructure and properties of WC-Bronze-Ni-Mn based impregnated diamond composites were investigated. Results showed that bending strength of matrix samples increased up to approximately 20% upon nano-WC addition, while densification and hardness fluctuate slightly. The grinding ratio of impregnated diamond composites increased significantly by about 100% due to nano-WC addition. The strengthening mechanism was proposed in detail. The related effects of bending strength, densification and diamond retention capabilities on wear resistance of diamond composites were revealed. WC-bronze impregnated diamond composite with 2.8 wt% nano-WC exhibited an optimal overall performance, thus having potential to apply to further diamond tools.

**Author Contributions:** B.L. and S.L. conceived and designed the experiments; S.L. and Z.H. performed the experiments; Q.M. and X.Z. analyzed the data; X.C. contributed analysis tools; S.L. wrote the paper.

**Funding:** This work is funded by the Science and Technology project of Jilin Province Education Department (JJKH20180087KJ) and the National Natural Science Foundation of China (41572357).

**Conflicts of Interest:** The authors declare no conflict of interest.

#### References

1. Tönshoff, H.K.; Hillmann, A.H.; Asche, J. Diamond tools in stone and civil engineering industry: Cutting principles, wear and applications. *Diam. Relat. Mater.* **2002**, *250*, 103–109. [[CrossRef](#)]
2. Boland, J.N.; Li, X.S. Microstructural Characterisation and Wear Behaviour of Diamond Composite Materials. *Materials* **2010**, *3*, 1390–1419. [[CrossRef](#)]
3. Zhao, X.; Duan, L. A Review of the Diamond Retention Capacity of Metal Bond Matrices. *Metals* **2018**, *8*, 307. [[CrossRef](#)]
4. Konstanty, J.S.; Baczek, E.; Romanski, A.; Tyrala, D. Wear-resistant iron-based Mn–Cu–Sn matrix for sintered diamond tools. *Powder Metall.* **2017**, *61*, 43–49. [[CrossRef](#)]
5. Artini, C.; Muolo, M.L.; Passerone, A. Diamond–metal interfaces in cutting tools: A review. *J. Mater. Sci.* **2011**, *47*, 3252–3264. [[CrossRef](#)]
6. Dai, H.; Wang, L.; Zhang, J.; Liu, Y.; Wang, Y.; Wang, L.; Wan, X. Iron based partially pre-alloyed powders as matrix materials for diamond tools. *Powder Metall.* **2015**, *58*, 83–86. [[CrossRef](#)]
7. Sun, Y.; Wu, H.; Li, M.; Meng, Q.; Gao, K.; Lu, X.; Liu, B. The Effect of ZrO<sub>2</sub> Nanoparticles on the Microstructure and Properties of Sintered WC-Bronze-Based Diamond Composites. *Materials* **2016**, *9*, 343. [[CrossRef](#)] [[PubMed](#)]
8. Li, M.; Sun, Y.H.; Dong, B.; Wu, H.D.; Gao, K. Study on effects of CNTs on the properties of WC-based impregnated diamond matrix composites. *Mater. Res. Innov.* **2015**, *19*, 59–63. [[CrossRef](#)]
9. Sun, Y.C.; Liu, Y.B. *Diamond Tool and Metallurgical Technology*; China Construction Materials Press: Beijing, China, 1999.
10. Di Ilio, A.; Togna, A. A theoretical wear model for diamond tools in stone cutting. *Int. J. Mach. Tools Manuf.* **2003**, *43*, 1171–1177. [[CrossRef](#)]
11. Wang, Z.; Zhang, Z.; Sun, Y.; Gao, K.; Liang, Y.; Li, X.; Ren, L. Wear behavior of bionic impregnated diamond bits. *Tribol. Int.* **2016**, *94*, 217–222. [[CrossRef](#)]
12. Ersoy, A.; Buyuksagic, S.; Atici, U. Wear characteristics of circular diamond saws in the cutting of different hard abrasive rocks. *Wear* **2005**, *258*, 1422–1436. [[CrossRef](#)]
13. Levashov, E.; Kurbatkina, V.; Alexandr, Z. Improved Mechanical and Tribological Properties of Metal-Matrix Composites Dispersion-Strengthened by Nanoparticles. *Materials* **2009**, *3*, 97–109. [[CrossRef](#)]

14. Casati, R.; Vedani, M. Metal Matrix Composites Reinforced by Nano-Particles—A Review. *Metals* **2014**, *4*, 65–83. [[CrossRef](#)]
15. Zhou, Y.M.; Zhang, F.L.; Wang, C.Y. Effect of Ni–Al SHS reaction on diamond grit for fabrication of diamond tool material. *Int. J. Refract. Met. Hard Mater.* **2010**, *28*, 416–423. [[CrossRef](#)]
16. Spriano, S.; Chen, Q.; Settineri, L.; Bugliosi, S. Low content and free cobalt matrixes for diamond tools. *Wear* **2005**, *259*, 1190–1196. [[CrossRef](#)]
17. Li, M.; Sun, Y.; Meng, Q.; Wu, H.; Gao, K.; Liu, B. Fabrication of Fe-Based Diamond Composites by Pressureless Infiltration. *Materials* **2016**, *9*, 1006. [[CrossRef](#)] [[PubMed](#)]
18. Uemura, M. An analysis of the catalysis of Fe, Ni or Co on the wear of diamonds. *Tribol. Int.* **2004**, *37*, 887–892. [[CrossRef](#)]
19. Narulkar, R.; Bukkapatnam, S.; Raff, L.M.; Komanduri, R. Graphitization as a precursor to wear of diamond in machining pure iron: A molecular dynamics investigation. *Comput. Mater. Sci.* **2009**, *45*, 358–366. [[CrossRef](#)]
20. Sidorenko, D.A.; Zaitsev, A.A.; Kirichenko, A.N.; Levashov, E.A.; Kurbatkina, V.V.; Loginov, P.A.; Rupasov, S.I.; Andreev, V.A. Interaction of diamond grains with nanosized alloying agents in metal–matrix composites as studied by Raman spectroscopy. *Diam. Relat. Mater.* **2013**, *38*, 59–62. [[CrossRef](#)]
21. Sidorenko, D.; Mishnaevsky, L.; Levashov, E.; Loginov, P.; Petrzhik, M. Carbon nanotube reinforced metal binder for diamond cutting tools. *Mater. Des.* **2015**, *83*, 536–544. [[CrossRef](#)]
22. Zaitsev, A.A.; Sidorenko, D.A.; Levashov, E.A.; Kurbatkina, V.V.; Rupasov, S.I.; Andreev, V.A.; Sevast'yanov, P.V. Development and application of the Cu-Ni-Fe-Sn-based dispersion-hardened bond for cutting tools of superhard materials. *J. Superhard Mater.* **2012**, *34*, 270–280. [[CrossRef](#)]
23. Loginov, P.; Mishnaevsky, L.; Levashov, E.; Petrzhik, M. Diamond and cBN hybrid and nanomodified cutting tools with enhanced performance: Development, testing and modelling. *Mater. Des.* **2015**, *88*, 310–319. [[CrossRef](#)]
24. Zaitsev, A.A.; Sidorenko, D.A.; Levashov, E.A.; Kurbatkina, V.V.; Andreev, V.A.; Rupasov, S.I.; Sevast'yanov, P.V. Diamond tools in metal bonds dispersion-strengthened with nanosized particles for cutting highly reinforced concrete. *J. Superhard Mater.* **2011**, *32*, 423–431. [[CrossRef](#)]
25. Loginov, P.A.; Sidorenko, D.A.; Levashov, E.A.; Petrzhik, M.I.; Bychkova, M.Y.; Mishnaevsky, L. Hybrid metallic nanocomposites for extra wear-resistant diamond machining tools. *Int. J. Refract. Met. Hard Mater.* **2018**, *71*, 36–44. [[CrossRef](#)]
26. Tjong, S.C. Novel Nanoparticle-Reinforced Metal Matrix Composites with Enhanced Mechanical Properties. *Adv. Eng. Mater.* **2007**, *9*, 639–652. [[CrossRef](#)]
27. Kamyar, S.; Mohammad, M.A.; Bhargav, P.; Minoos, N. Periodical patterning of a fully tailored nanocarbon on CNT for fabrication of thermoplastic composites. *Compos. A* **2018**, *107*, 304–314.
28. Karbalaeei, A.M.; Rajabi, S.; Shirvanimoghaddam, K. Wear and friction behavior of nanosized Formula and Formula particle-reinforced casting A356 aluminum nanocomposites: A comparative study focusing on particle capture in matrix. *J. Compos. Mater.* **2015**, *49*, 3665–3681. [[CrossRef](#)]
29. Myalska, H.; Swadźba, R.; Rozmus, R.; Moskal, G.; Wiedermann, J.; Szymański, K. STEM analysis of WC-Co coatings modified by nano-sized TiC and nano-sized WC addition. *Surf. Coat. Technol.* **2017**, *318*, 279–287. [[CrossRef](#)]
30. Mauro, P.; Sasa, B. On the Properties of WC/SiC Multilayers. *Appl. Sci.* **2018**, *8*, 571. [[CrossRef](#)]
31. Kurllov, A.S.; Rempel, A.A. Effect of WC nanoparticle size on the sintering temperature, density, and microhardness of WC-8 wt % Co alloys. *Inorg. Mater.* **2009**, *45*, 380–385. [[CrossRef](#)]
32. Zhang, Z.; Chen, D. Consideration of Orowan strengthening effect in particulate-reinforced metal matrix nanocomposites: A model for predicting their yield strength. *Scr. Mater.* **2006**, *54*, 1321–1326. [[CrossRef](#)]
33. Zhang, Z.; Chen, D.L. Contribution of Orowan strengthening effect in particulate-reinforced metal matrix nanocomposites. *Mater. Sci. Eng. A* **2008**, *483–484*, 148–152. [[CrossRef](#)]
34. Vaidya, R.U.; Chawla, K.K. Thermal expansion of metal-matrix composites. *Compos. Sci. Technol.* **1994**, *50*, 13–22. [[CrossRef](#)]

